

A Tetranuclear, Macrocyclic 3d–4f Complex Showing Single-Molecule Magnet Behavior

Humphrey L. C. Feltham,[†] Rodolphe Clérac,^{‡,§} Annie K. Powell,^{*,†} and Sally Brooker^{*,†}

[†]Department of Chemistry and MacDiarmid Institute, University of Otago, P.O. Box 56, Dunedin 9054, New Zealand

[‡]CNRS, UPR 8641, Centre de Recherche Paul Pascal (CRPP), Equipe “Matériaux Moléculaires Magnétiques”, 115 avenue du Dr. Albert Schweitzer, Pessac F-33600, France

[§]Université de Bordeaux, UPR 8641, Pessac F-33600, France

[†]Institut für Anorganische Chemie, Karlsruher Institut für Technologie, Engesserstrasse 15 Geb. 30.45, 76131 Karlsruhe, Germany

S Supporting Information

ABSTRACT: $[\text{Cu}^{\text{II}}_3\text{Tb}^{\text{III}}(\text{L}^{\text{Pr}})(\text{NO}_3)_2(\text{MeOH})(\text{H}_2\text{O})_2](\text{NO}_3) \cdot 3\text{H}_2\text{O}$ is a rare example of a 3d–4f single-molecule magnet prepared using a macrocyclic ligand: at low T , it exhibits frequency-dependent alternating-current susceptibility, indicative of slow relaxation of the magnetization.

Single-molecule magnets (SMMs) are complexes that have the capacity to act as a magnet at the molecular level. After an SMM is magnetized under an external magnetic field at low temperatures, the relative stability of the two spin ground states ($\pm S_T$) over intermediary spin states prevents the rapid loss of the magnetization in zero direct-current (dc) field.¹ The anisotropy of the spin states induces slow dynamics, such that reorientation of the magnetization requires overcoming an energy barrier and thus becomes sluggish. Attempts to maximize the barrier can be foiled by quantum tunneling through it: to minimize this, it has been proposed that 3-fold symmetry is desirable.² In SMMs containing lanthanide ions, the crucial magnetic anisotropy is the result of the spin states being made nondegenerate by certain coordination environment symmetries.

SMMs containing a single lanthanide ion were first prepared by Ishikawa et al. using phthalocyanine macrocycles.³ Slow relaxation of the magnetization has since been demonstrated for a range of complexes with just one lanthanide ion, including those based on polyoxometallates (including metallomacrocycles),⁴ Schiff bases,⁵ radicals⁶ and ketones.⁷ Current efforts to identify SMMs with higher blocking temperatures tend to be focused on combining lanthanide metal ions with transition-metal ions^{8,9} rather than on producing multiple 4f complexes because the exchange interaction between 4f ions is inherently weak.¹⁰

Inspired by the macrocyclic systems prepared from dialdehyde 1,4-diformyl-2,3-dihydroxybenzene (**1**)¹¹ by Akine and Nabeshima¹² and Frischmann and MacLachlan,¹³ we have prepared new [3 + 3] Schiff-base macrocycles derived from this head unit, with the aim of systematically examining the magnetic properties of families of 3d–4f $M_3\text{Ln}$ complexes (Figure 1). The provision of binding sites of different sizes and donor types greatly facilitates the formation of the desired $M_3\text{Ln}$ complexes (cf. M_4 to M_{12} aggregates using related *acyclic* multidentate ligand analogues¹⁴). Encapsulating the $M_3\text{Ln}$ core with the

organic macrocycle also provides *stability* (macrocyclic effect), which, in turn, facilitates fine tuning of the metal ion environments (vary R and n , see Figure 1) and solubility (vary R). In the first family, $[\text{Zn}^{\text{II}}_3\text{Ln}^{\text{III}}(\text{L}^{\text{Pr}})]^{3+}$, we found that the $\text{Zn}^{\text{II}}_3\text{Dy}^{\text{III}}$ complex displayed slow relaxation of the magnetization under an applied dc field.⁹

With this promising result in hand, we are now replacing the diamagnetic Zn^{II} ions by paramagnetic transition-metal ions because this may enhance the SMM energy barrier. While the desired complexes could, in principle, be prepared by transmetalation of the Zn_3Ln complexes, it appeared to us that, like Zn^{II} , Cu^{II} , in conjunction with a Ln^{III} ion, should template the $(\text{L}^{\text{Pr}})^{6-}$ macrocycle, facilitating direct access to the complexes of interest.

Template synthesis followed by recrystallization gave $[\text{Cu}^{\text{II}}_3\text{Tb}^{\text{III}}(\text{L}^{\text{Pr}})(\text{NO}_3)_2(\text{MeOH})(\text{H}_2\text{O})_2](\text{NO}_3) \cdot 3\text{H}_2\text{O}$ (**2**) as a brown powder, in 45% yield, which was characterized by elemental analysis, mass spectrometry, and IR absorption spectroscopy (see the Supporting Information, SI).

Single crystals of $[\text{Cu}^{\text{II}}_3\text{Tb}^{\text{III}}(\text{L}^{\text{Pr}})(\text{NO}_3)_2(\text{MeOH})_3](\text{NO}_3)$ suitable for X-ray crystallography were obtained by vapor diffusion of diethyl ether into a methanol solution of **2**. The structure determination confirmed that the macrocycle coordinates one Tb^{III} ion in the central, larger O_6 cavity and three smaller Cu^{II} ions in the outer N_2O_2 sites, with approximate 3-fold symmetry (Figure 2). As a result, the macrocycle adopts a slightly curved conformation. All three Cu^{II} ions possess a square-pyramidal geometry with a long apical bond. One of the Cu^{II} ions is distorted toward trigonal bipyramidal (trigonality factor¹⁵ $\tau = 0.17$), whereas the other two are almost perfectly regular square pyramids ($\tau < 0.02$). One of the three nitrate ions is bound to the Tb^{III} ion in a bidentate fashion, the second is bound to a Cu^{II} ion via one oxygen atom, while the third is not bound. The complexes pack in weakly connected pairs in the lattice (see Figure S1 in the SI; $O30 \cdots O50$ 2.74 Å hydrogen bond and $O31 \cdots \text{Cu}2A$ 2.92 Å weak axial interaction): the Tb^{III} ions in neighboring complexes are 8.59 Å apart.

At room temperature, the χT product of **2** (Figure 3) is $13 \text{ cm}^3 \text{ K mol}^{-1}$, in good agreement with the expected value of $12.9 \text{ cm}^3 \text{ K mol}^{-1}$ for 3 Cu^{II} ($S = 1/2$; $g = 2.0$; $C = 0.375 \text{ cm}^3 \text{ K mol}^{-1}$) and 1 Tb^{III} ($S = 3$, $L = 3$, 7F_6 , $g = 3/2$, $C = 11.815 \text{ cm}^3 \text{ K mol}^{-1}$).

Received: February 20, 2011

Published: April 08, 2011

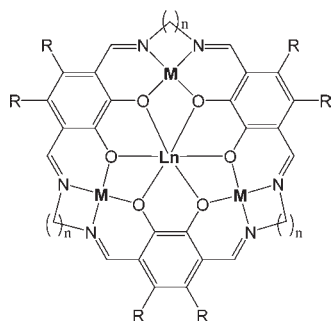


Figure 1. Hexamine [3 + 3] macrocycle ($L^{\text{Pr}})^{6-}$ used in this work has $R = \text{H}$, $n = 3$. It is prepared and complexed in situ (i.e., not isolated).

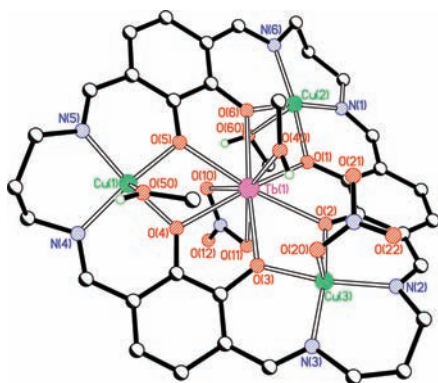


Figure 2. Crystal structure of $[\text{Cu}^{\text{II}}_3\text{Tb}^{\text{III}}(L^{\text{Pr}})(\text{NO}_3)_2(\text{MeOH})_3] \cdot (\text{NO}_3)$. For clarity, the disorder of the propylene linkage, non-acidic hydrogen atoms, and non-coordinated $[\text{NO}_3]^-$ anion have been omitted.

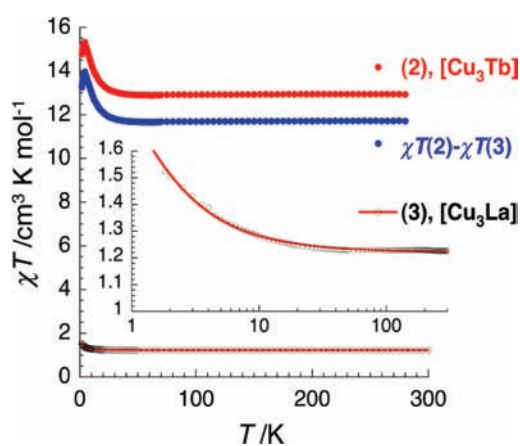


Figure 3. Temperature dependence of the χT product per $[\text{Cu}_3\text{Ln}]$ unit, measured on polycrystalline samples of **2** and **3** between 1.8 and 300 K under 1000 Oe. Inset: χT versus T plot on a semilogarithmic scale for **3**. The solid line represents the best fit described in the text.

Upon lowering of the temperature, the χT product is roughly constant down to 50 K before exhibiting a slow increase, reaching a maximum of $15.3 \text{ cm}^3 \text{ K mol}^{-1}$ at around 3.5 K and then decreasing to a minimum value at 1.8 K of $14.7 \text{ cm}^3 \text{ K mol}^{-1}$, indicating the presence of magnetic anisotropy or weak inter-complex antiferromagnetic interactions (Figure S1 in the SI).

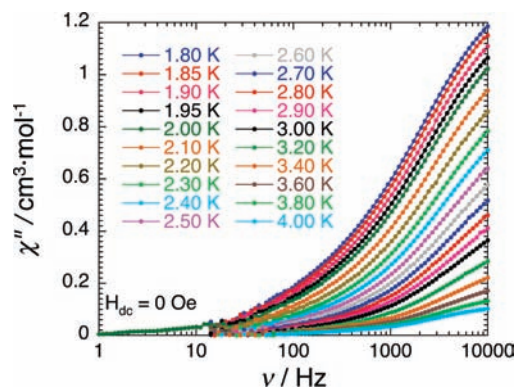


Figure 4. Frequency dependence of the out-of-phase component of the ac susceptibility of **2** at temperatures indicated with 1 Oe (at all temperatures except 2 K) or 3 Oe (at 2 K) of ac field modulation and in zero dc field.

In order to understand the magnetic behavior of **2**, the contribution from the Cu^{II} ions was determined by measuring the magnetic properties of the analogous La^{III} complex, $[\text{Cu}^{\text{II}}_3\text{La}^{\text{III}}(L^{\text{Pr}})(\text{NO}_3)_2(\text{MeOH})_2(\text{H}_2\text{O})](\text{NO}_3) \cdot \text{MeOH}$ (**3**; see the SI), which contains a diamagnetic La^{III} ion in place of the paramagnetic Tb^{III} ion. At room temperature the χT product for **3** (Figure 3) is $1.2 \text{ cm}^3 \text{ K mol}^{-1}$, in good agreement with the expected value of $1.125 \text{ cm}^3 \text{ K mol}^{-1}$ for three Cu^{II} ions ($g_{\text{Cu}} = 2$) and one diamagnetic La^{III} ion. When the temperature is lowered, the χT product is roughly constant down to 50 K, before exhibiting a slow increase and reaching a maximum value of $1.5 \text{ cm}^3 \text{ K mol}^{-1}$ at 1.8 K. The absence of a rapid drop in the χT product at very low temperature indicates an absence of significant magnetic anisotropy or intercomplex antiferromagnetic interactions in **3**.

The temperature dependence of the susceptibility for **3** was modeled using a simple symmetrical $S = 1/2$ triangle model as a first approximation (Figure S2 in the SI). In keeping with the structural motif, the Heisenberg spin Hamiltonian can be written as $H = -J(S_1 \cdot S_2 + S_1 \cdot S_3 + S_2 \cdot S_3)$. From this model, application of the van Vleck equation¹⁶ allows the determination of the low-field ($\mu_{\text{B}}H/k_{\text{B}}T \ll 1$) analytical expression of the magnetic susceptibility.¹⁷ An excellent fit of the experimental data is obtained with this theoretical susceptibility, with $J/k_{\text{B}} = +0.5(1) \text{ K}$ and $g = 2.08(2)$, down to 1.8 K (Figure 3). This result indicates a weak ferromagnetic coupling between the Cu^{II} ions within **3** that thus possesses an $S_{\text{T}} = 3/2$ spin ground state.

Subtraction of the experimental χT versus T data for **3** from that obtained for **2** removes the contributions from the $\text{Cu}^{\text{II}}-\text{Cu}^{\text{II}}$ interactions and $[\text{Cu}_3]$ paramagnetism, allowing the nature of the magnetic interactions between the Cu^{II} and Tb^{III} ions to be probed. As shown in Figure 3, the difference plot is roughly constant down to 50 K and then increases at lower temperatures, confirming the ferromagnetic nature of the $\text{Cu}^{\text{II}}-\text{Tb}^{\text{III}}$ interaction (note that a decrease of the χT product upon lowering of the temperature should be observed if the intrinsic spin-orbit coupling of the Tb^{III} ion was dominating the magnetic properties).

The field dependence of the magnetization of **2** was also measured at various temperatures to check for hysteresis, i.e., slow relaxation of the magnetization (Figure S3 in the SI). Below 10 K, the magnetization increases rapidly at low field strength before a gradual linear increase. The magnetization does not

saturate but reaches $8.0 \mu_B$ at 1.8 K in a field of 70 kOe. The high-field linear variation of the magnetization highlights the presence of a significant magnetic anisotropy, as was expected for the Tb^{III} ion present in this system. Moreover, the plot of M versus H/T (Figure S3 in the SI) at different fields shows that the curves are not all superposable on a single master curve, further confirming the presence of magnetic anisotropy. No hysteresis for the M versus H data was observed above 1.8 K with sweep rates of $100\text{--}200 \text{ Oe min}^{-1}$.

Nevertheless, the behavior of **2** in an alternating-current (ac) magnetic field was measured to check for the presence of slow relaxation of the magnetization at shorter time scales. Below approximately 5 K, the out-of-phase component of ac susceptibility (χ'') becomes nonzero and exhibits a frequency dependence (as it does the in-phase component), as is characteristic of an SMM (Figures S4 and S5 in the SI). The signal reaches around $1.2 \text{ cm}^3 \text{ mol}^{-1}$ at 10 kHz and 2 K but is still increasing at this point and so the maximum of the plot is not visible within the temperature limits of the measurement.

The ac susceptibility as a function of the frequency at different temperatures has also been measured in order to follow, if possible, the relaxation (Figure 4). Unfortunately, the maximum does not appear in the frequency limit of these measurements (10 kHz), which precludes the determination of the τ versus $1/T$ data and a fit of this to an Arrhenius law. From Figure 4, it appears clearly that the relaxation mode is located slightly above 10 kHz at 1.8 K. This gives a rough idea of the relaxation time (τ), which is around $1 \times 10^{-5} \text{ s}$ at 1.8 K, so τ is relatively short.

When ac susceptibility measurements on **2** were conducted in the presence of external dc fields of different strengths at 1.9 K (to suppress a possible fast ground state quantum tunneling of the magnetization), the maxima of the χ'' versus ν data did not shift to within the frequency window of the measurement (Figure S6 in the SI). Indeed, relaxation of the magnetization in **2** is not slowed by the applied dc field, suggesting that quantum tunneling of magnetization is not an efficient relaxation pathway above 1.9 K.

In conclusion, we have prepared a tetranuclear $Cu^{II}\text{--}Tb^{III}$ complex that shows slow relaxation of the magnetization in zero dc field, a property that is absent in **3** and is very weak in the Zn_3Dy analogue.⁹ Complex **2** is the second example in this new class of 3d–4f SMMs where metal ions are hosted by a single organic macrocycle that provides control, solubility, tuneability, and stability. The incorporation of synthetically far more challenging, but magnetically very interesting, 3d metal ions is our next target, as we aim to continue to improve the SMM properties of this new family of 3d–4f complexes in a systematic and rational manner.

ASSOCIATED CONTENT

S Supporting Information. Experimental procedure for the preparation of **2** and **3**, crystallographic refinement details (CCDC 796813) for $[Cu^{II}_3Tb^{III}(L^{Pr})(NO_3)_2(MeOH)_3](NO_3)$, a figure showing weak dimer formation in the crystal lattice, and additional magnetic data. This material is available free of charge via the Internet at <http://pubs.acs.org>.

AUTHOR INFORMATION

Corresponding Author

*E-mail: sbrooker@chemistry.otago.ac.nz (S.B.), annie.powell@kit.edu (A.K.P.).

ACKNOWLEDGMENT

This work was supported by grants from the University of Otago and the MacDiarmid Institute for Advanced Materials and Nanotechnology. We also thank the University of Bordeaux, CNRS, Region Aquitaine, GIS Advanced Materials in Aquitaine (COMET Project), Dumont d'Urville NZ-France Science & Technology Support Programme (Program 23793PH), and Julius von Haast Fellowship Fund (RSNZ) for financial support.

REFERENCES

- (1) Aromí, G.; Brechin, E. K. *Struct. Bonding (Berlin)* **2006**, *122*, 1–67. Gatteschi, D.; Sessoli, R. *Angew. Chem., Int. Ed.* **2003**, *42*, 268–297.
- (2) Glaser, T. *Chem. Commun.* **2011**, *47*, 116–130. Freedman, D. E.; Harman, W. H.; Harris, T. D.; Long, G. J.; Chang, C. J.; Long, J. R. *J. Am. Chem. Soc.* **2010**, *132*, 1224–1225.
- (3) Ishikawa, N.; Sugita, M.; Ishikawa, T.; Koshihara, S.-y.; Kaizu, Y. *J. Am. Chem. Soc.* **2003**, *125*, 8694–8695.
- (4) Al-Damen, M. A.; Cardona-Serra, S.; Clemente-Juan, J. M.; Coronado, E.; Gaita-Arino, A.; Martí-Gastaldo, C.; Luis, F.; Montero, O. *Inorg. Chem.* **2009**, *48*, 3467–3479.
- (5) Li, D.-P.; Wang, T.-W.; Li, C.-H.; Liu, D.-S.; Li, Y.-Z.; You, X.-Z. *Chem. Commun.* **2010**, *46*, 2929–2931.
- (6) Wang, X.-L.; Li, L.-C.; Liao, D.-Z. *Inorg. Chem.* **2010**, *49*, 4735–4737. Zhou, N.; Ma, Y.; Wang, C.; Xu, G. F.; Tang, J.-K.; Xu, J.-X.; Yan, S.-P.; Cheng, P.; Lia, L.-C.; Liao, D.-Z. *Dalton Trans.* **2009**, 8489–8492.
- (7) Jiang, S.-D.; Wang, B.-W.; Su, G.; Wang, Z.-M.; Gao, S. *Angew. Chem., Int. Ed.* **2010**, *122*, 7610–7613.
- (8) Papatrifaftyllopoulou, C.; Wernsdorfer, W.; Abboud, K. A.; Christou, G. *Inorg. Chem.* **2011**, *50*, 421–423. Yamaguchi, T.; Costes, J.-P.; Kishima, Y.; Kojima, M.; Sunatsuki, Y.; Brefuel, N.; Tuchagues, J.-P.; Vendier, L.; Wernsdorfer, W. *Inorg. Chem.* **2010**, *49*, 9125–9135. Chilton, N. F.; Langley, S. K.; Moubaraki, B.; Murray, K. S. *Chem. Commun.* **2010**, *46*, 7787–7789. Baskar, V.; Gopal, K.; Helliwell, M.; Tuna, F.; Wernsdorfer, W.; Winpenny, R. E. P. *Dalton Trans.* **2010**, 39, 4747–4750. Boron, T. T.; Kampf, J. W.; Pecoraro, V. L. *Inorg. Chem.* **2010**, *49*, 9104–9106. Novitchi, G.; Wernsdorfer, W.; Chibotaru, L. F.; Costes, J.-P.; Anson, C. E.; Powell, A. K. *Angew. Chem., Int. Ed.* **2009**, *48*, 1614–1619. Andruh, M.; Costes, J.-P.; Diaz, C.; Gao, S. *Inorg. Chem.* **2009**, *48*, 3342–3359. Chandrasekhar, V.; Pandian, B. M.; Vittal, J. J.; Clérac, R. *Inorg. Chem.* **2009**, *48*, 1148–1157. Aronica, C.; Chastanet, G.; Pilet, G.; Guennic, B. L.; Robert, V.; Wernsdorfer, W.; Luneau, D. *Inorg. Chem.* **2007**, *46*, 6108–6119.
- (9) Feltham, H. L. C.; Lan, Y.; Klöwer, F.; Ungur, L.; Chibotaru, L. F.; Powell, A. K.; Brooker, S. *Chem.—Eur. J.* **2011**, *17*, 4362–4265, and cover feature.
- (10) Sessoli, R.; Powell, A. K. *Coord. Chem. Rev.* **2009**, *253*, 2328–2341.
- (11) Feltham, H. L. C.; Brooker, S. *Coord. Chem. Rev.* **2009**, *253*, 1458–1475. Nabeshima, T. *Bull. Chem. Soc. Jpn.* **2010**, *83* (9), 969–991. Kleij, A. W. *Chem.—Eur. J.* **2008**, *14*, 10520–10529.
- (12) Akine, S.; Nabeshima, T. *Dalton Trans.* **2009**, 10395–10408. Akine, S.; Sunaga, S.; Taniguchi, T.; Miyazaki, H.; Nabeshima, T. *Inorg. Chem.* **2007**, *46*, 2959–2961.
- (13) Frischmann, P. D.; MacLachlan, M. J. *Comments Inorg. Chem.* **2008**, *29*, 26–45. Frischmann, P. D.; Jiang, J.; Hui, J. K. H.; Grzybowski, J. J.; MacLachlan, M. J. *Org. Lett.* **2008**, *10* (6), 1255–1258.
- (14) Feltham, H. L. C.; Clérac, R.; Brooker, S. *Dalton Trans.* **2009**, 2965–2973 and references cited therein.
- (15) Addison, A. W.; Rao, T. N.; Reedijk, J.; van Rijn, J.; Verschoor, G. C. *J. Chem. Soc., Dalton Trans.* **1984**, 1349–1356.
- (16) van Vleck, J. H. *The Theory of Electric and Magnetic Susceptibility*; Oxford University Press: Oxford, U.K., 1932.
- (17) Murugesu, M.; Clérac, R.; Anson, C. E.; Powell, A. K. *J. Phys. Chem. Solids* **2004**, *65*, 667–676.
- (18) Feltham, H. L. C.; Clérac, R.; Powell, A. K.; Brooker, S., unpublished results.